https://doi.org/10.46813/2024-153-066

POSITRON SOURCES OF THE MULTIFUNCTIONAL ACCELERATOR COMPLEX OF NSC KIPT

P.I. Gladkikh, I.S. Guk, G.D. Kovalenko, O.O. Parkhomenko, S.I. Prokhorets, E.V. Rudychev
National Science Center “Kharkiv Institute of Physics and Technology”,
Kharkiv, Ukraine
E-mail: guk@kipt.kharkov.ua

The possibility of producing positron beams using an electron recycler, the conceptual design of which is being developed at KIPT, is considered. The positron flux after the tantalum converter was estimated. The efficiency of the process of injection and acceleration of positrons to 181 and 356 MeV for high-energy physics experiments was calculated. The characteristics of the beam for use in structural studies of solid state physics are considered.

PACS: 41.75.Ht, 25.20.-x.

INTRODUCTION

Experimental and theoretical studies of the interaction of electrons and positrons with matter began at KIPT in 1970.

The decisive factor in the development of these works was the creation of low-divergence, monochromatic and intense electron and positron beams at linear accelerators at 300 MeV and 2 GeV [1].

One of the important aspects that attract the attention of theory and experiment to the process of interaction of electrons and positrons with single crystals is the possibility of generating gamma-ray beams with a significantly higher spectral-angle density compared to the braking radiation of charged particles in an amorphous target. This feature of the interaction of charged particles with crystals has been reflected in a large number of original papers and a number of reviews. Many experimental works performed in this area are devoted to the study of various aspects of the physics of the interaction of charged particles with single crystals with different atomic numbers (C, Si, Ge, Nb, W), crystal thickness, and orientation of crystallographic axes and planes relative to the direction of the primary beam of charged particles [2–9]. As a result of experimental and theoretical studies, the understanding of the mechanism of interaction of charged particles with single crystals and amorphous substances has been significantly expanded. However, from the point of view of practical applications (in particular, the creation of sources of intense directed gamma radiation), a number of areas remain insufficiently studied. Therefore, research remains relevant [10]:

- the processes of converting electron and positron energy into gamma radiation energy, aimed at finding ways to increase the efficiency of gamma radiation generation based on single-crystal converters;
- passage of high-energy electrons through the crystal along one of the crystallographic axes (oriented crystal), since the spectral density of gamma radiation of electrons in this case has the most pronounced anomalies, and the total loss of radiation energy of electrons is maximal;
- behavior of different energy regions in the electron gamma-ray spectrum with the crystal thickness;
- polarization properties of gamma radiation in the region of several tens of MeV, i.e., in the energy range characteristic of radiation from reactions in the giant resonance region;
- on-the-fly annihilation of positrons in single crystals to create more efficient sources of quasi-monochromatic gamma-ray sources for use in nuclear and high-energy physics;
- transmutation doping process of especially pure silicon with aluminum in a gamma-ray beam;
- emission properties of amorphous and single crystalline substances during the passage of relativistic electrons and positrons.

The second area of widespread use of positron beams is the method of positron annihilation in the study of the defective structure of solids, liquids, and biological samples [11–14]. Various material defects, such as dislocations, grain boundaries, single or cluster vacancies, and voids, change the energy spectrum of emitted photons and positron lifetime in a characteristic way due to different distributions of the annihilating positron pulse and their concentration.

The most informative techniques are measuring the lifetime of positrons in matter and determining the angular distribution of photons. When these two techniques are used together, more detailed information about the electronic structure of a material can be obtained.

The study of the properties of materials, including structural steels used in nuclear reactors, is particularly relevant [14].

In recent years, the number of positron spectrometers in various research centers has been increasing dramatically. This is due to the fact that positron annihilation usually provides information about the structure of matter that is not available for study by other experimental methods. In addition, positron annihilation is one of the non-destructive research methods, i.e., its use does not exclude further study of the same object by other methods.

Along with isotopes, electron accelerators are also used as sources of positrons in annihilation techniques [13, 15, 16].

Let's consider what positron sources can be created with the help of a recirculator, the project of which is being developed at NSC KIPT [17].

1. PRODUCTION OF POSITRONS USING AN ELECTRON ACCELERATOR

1.1. POSITRON GENERATION

According to the review [18], the main way to produce positron beams for their further acceleration to high energy is the interaction of an electron beam with tantalum or tungsten targets. In the proposed recirculator injection structure [17], a beam with an energy of 29 MeV can be used for this purpose. It consists of the energy of the injector, which in the high charge mode can accelerate the beam up to 4 MeV with a charge in the bunch of 300 pC [19], and the energy increase to 25 MeV due to the superconducting accelerator module.

It is known that when using an electron accelerator, the source of positrons is bremsstrahlung emission. Positrons are generated by the formation of electron-positron pairs if the energy of the bremsstrahlung emission is greater than 1.02 MeV.

The modeling of the positron production process was performed using the Particle and Heavy Ion Transport code System (PHITS) program [20].

The characteristics of the electron beam were as follows. Beam energy 29 MeV. The beam is cylindrical with zero divergence. The transverse distribution of the beam corresponds to the Gaussian distribution. The beam root mean square size FWHM = 1 mm.

To study the distributions of bremsstrahlung emission and positrons as a function of thickness, the converter was assembled from 90 disks of 4 mm diameter and 0.2 mm thickness each. As shown in Fig. 1, the total thickness of the converter was 1.8 cm.

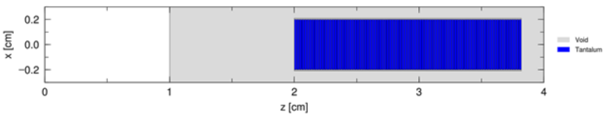

Fig. 1. Geometry of the tantalum converter

The spatial distribution of the bremsstrahlung emission around the target in the photon energy range from 1.02 to 29 MeV is shown in Fig. 2.

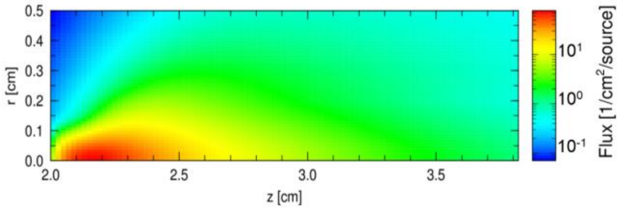

Fig. 2. Spatial distribution of bremsstrahlung emission

The spatial distribution of positrons produced by the photon beam is shown in Fig. 3.

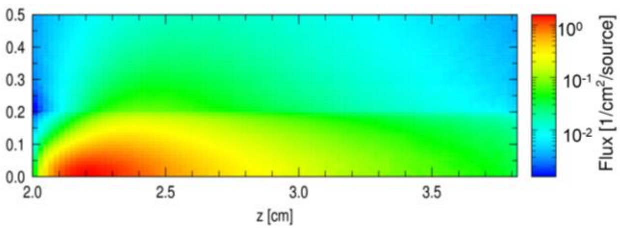

Fig. 3. Spatial distribution of positrons

The graph of bremsstrahlung emission outputs depending on the thickness of the converter is shown in Fig. 4.

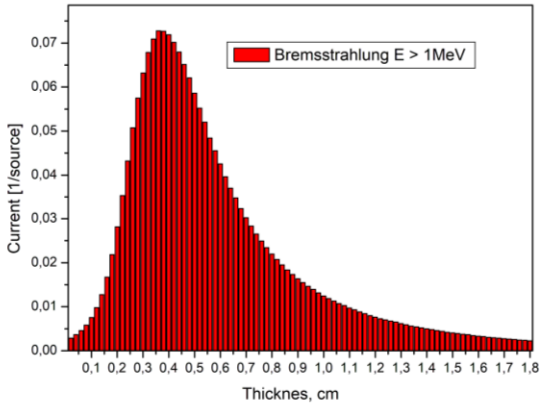

Fig. 4. bremsstrahlung emission output depending on the thickness of the converter

As can be seen from Figs. 2–4, the optimal converter thickness is close to 4 mm. For this thickness, we simulated the irradiation by an electron beam in the geometry shown in Fig. 5.

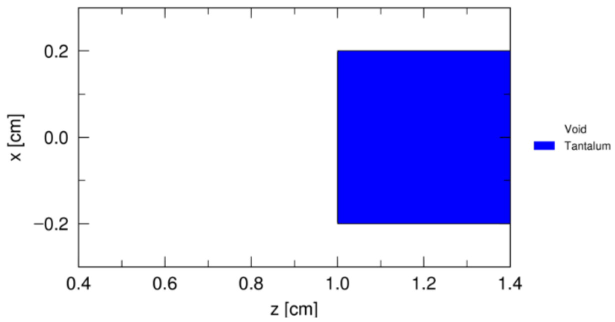

Fig. 5. Geometry of the optimal target

The trajectories of a continuous electron beam in this geometry are shown in Fig. 6. Electron energy range from 1.02 to 29 MeV.

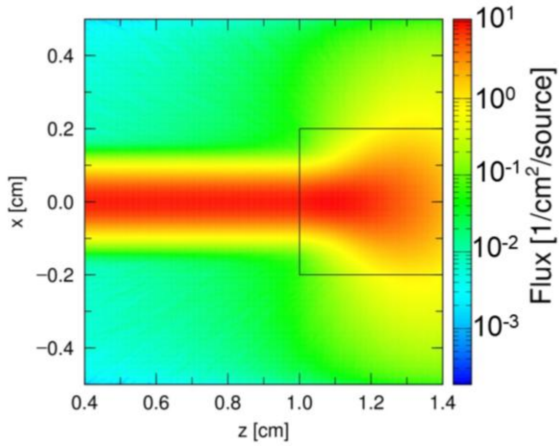

Fig. 6. Distribution of electrons around the target

The distribution of bremsstrahlung emission in the photon energy range from 1.02 to 29 MeV is shown in Fig. 7.

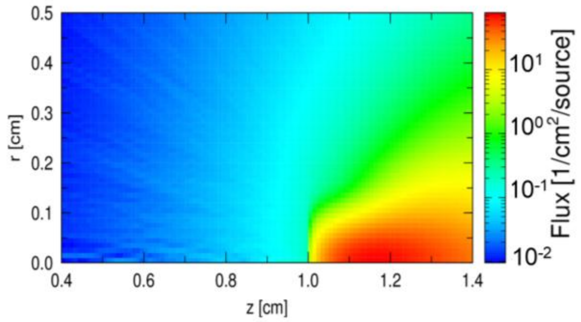

Fig. 7. Distribution of bremsstrahlung emission

The spatial distribution of positron production around the converter in the energy range from 1.02 to 29 MeV is shown in Fig. 8.

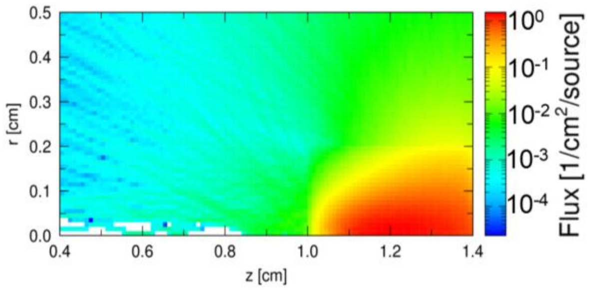

Fig. 8. Spatial distribution of positrons

The distribution of positrons by energy after the target is shown in Fig. 9.

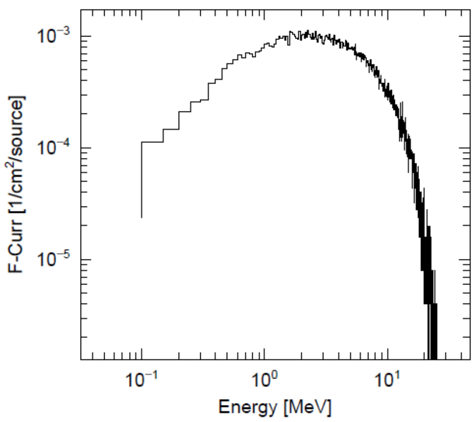

Fig. 9. Positron spectrum

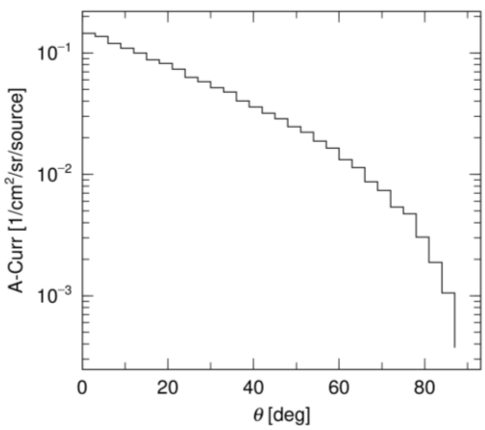

Fig. 10. Angular distribution of positrons after the converter

Fig. 10 shows the distribution of the beam by departure angles relative to the axis of the electron beam incident on the converter.

The electron beam in the accelerator [19] in the high charge mode in the bunch consists of 5 ps long clots with a charge of 300 pC. The distribution of positrons in the space around the converter at 22, 49, and 109 ps after the start of the interaction of the electron beam with the converter is shown in Figs. 11–13.

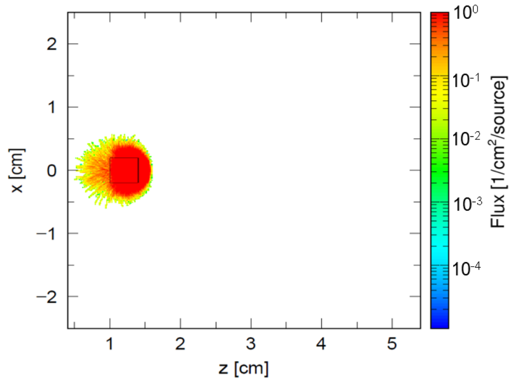

Fig. 11. Distribution after 22ps

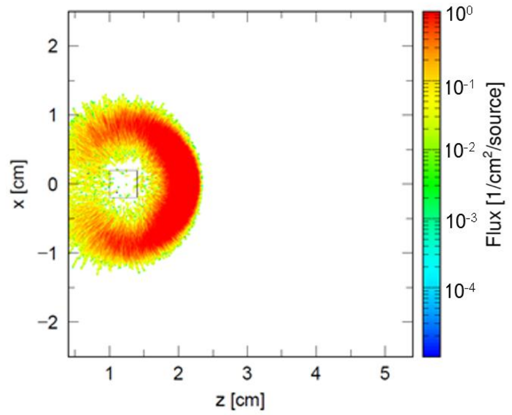

Fig. 12. Distribution after 49ps

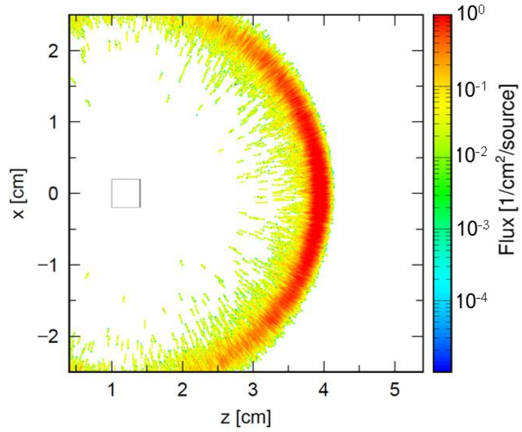

Fig. 13. Distribution through 109ps

1.2. POSITRON SOURCE FOR HIGH-ENERGY PHYSICS

Fig. 14 shows the scheme of the injection path on the recirculator [17]. The beam after the injector and accelerator section is focused by a triplets of quadrupole lenses. The dipole magnet BM1 rotates the beam, which is injected into the main correction structure of the recirculator through a system of five quadrupoles and the

BM2 magnet. The converter must be positioned in a straight line between the triplet and the BM1 magnet.

In the standard operating mode, the injection energy into the recycler is E_{iel} = 29 MeV, which, with the energy gain in the accelerating structures E_{acc} = 175 MeV, provides electron energies E_e = 204, 379, and 554 MeV after the first, second, and third passage of the beam through the accelerating structures, respectively. To change the beam energy at the outputs in the recirculator, it is necessary to synchronously and proportionally change the injection energy and energy gain in the accelerating structures. Then the beam orbit in the magnetic elements remains unchanged.

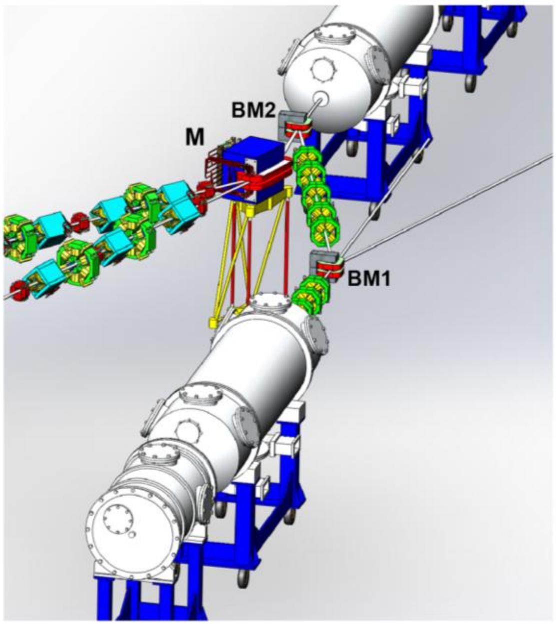

Fig. 14. Beam injection into the recirculator

For acceleration in the recycler, the positron injection energy E_{ipos} = 6 MeV was chosen. Due to the above-mentioned peculiarity of the recirculator structures, the use of the standard operating mode becomes unsuitable for accelerating positrons to high energies. In this mode, the positron energy after acceleration in the structures will be

$$E_{pos} = \frac{E_{ipos}}{E_{iel}}\left(E_{iel} + nE_{acc}\right) = 42.2,\ 78.4 \text{ and } 114.6 \text{ MeV}.$$

Here *n* is the number of passes by the beam of accelerating structures.

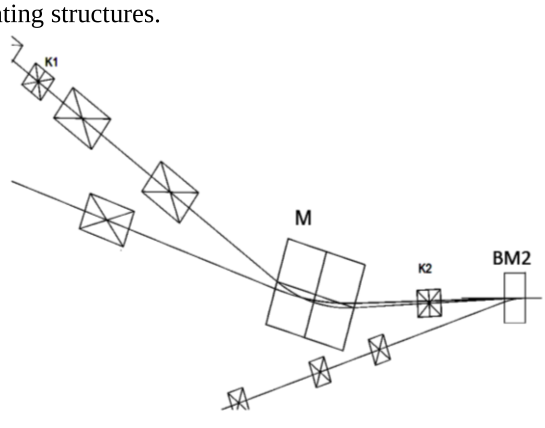

Fig. 15. End of the second arch of the first ring

In order to maximize the positron energy, it is proposed to use a local bump at the outlet of the second arch of the first ring (see Figs. 14–16).

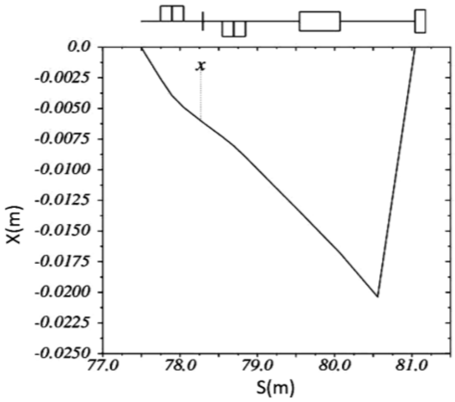

Fig. 16. Local bump

Failure to comply with the proportionality of the change in injection energy and energy gain in the accelerating structure leads to a distortion of the equilibrium orbit at the output of the second injection magnet (BM2 in Figs. 14 and 15) after the end of the beam rotation in the first ring. With the help of correctors K1 and K2, an orbital shift is created to compensate for the orbital deviation due to the disproportionate change in E_{ipos} and E_{acc}. The location of the correctors is optimized from the point of view of obtaining the minimum deviation of the equilibrium orbit in the bump area.

The described technique will produce positrons with energies

$E_1 = E_{ipos} + E_{acc} = 6 + 175 = 181$ MeV after the first pass of the accelerator structure and

$E_2 = E_{ipos} + 2 \cdot E_{acc} = 6 + 2 \cdot 175 = 356$ MeV after the second pass through this structure.

To form the beam in the injection channel, it is planned to install two collimators with a length of 250 mm and an aperture of ± 5 mm. The first collimator will be installed immediately after the positron converter, and the second will be placed in the dispersion section of the parallel transfer.

To obtain reliable characteristics of the beam passage through the injection channel and through the first ring of the recirculator, the phase volume of the beam for modeling its transportation was chosen as follows:

- transverse beam size (rms) $\sigma_x = \sigma_y$ = 2 mm;
- beam divergence $\sigma_{x'} = \sigma_{y'}$ = 25 mrad;
- particle energy range E_{ipos} = 6 ± 0.3 MeV.

Processing of the energy and angular spectra of the positrons selected in the simulation shows that the phase volume chosen for transportation contains approximately 1% of the generated positrons.

The above phase volume was simulated with 10,000 particles with a Gaussian distribution over coordinates truncated to 1σ. Fig. 17 shows the phase portraits of the beam in transverse planes at the exit of the BM2 injection magnet. Out of 10.000 particles, 220 particles (approximately 2%) pass through the injection channel after the converter.

The beam with an energy of 181 MeV after the first pass through the accelerating structure has the parameters shown in Fig. 18.

The beam with energy E_{pos} = 356 MeV after the second pass through the accelerating structure is shown in Fig. 19. Out of 10.000 particles after the converter, approximately 150 particles reached the output.

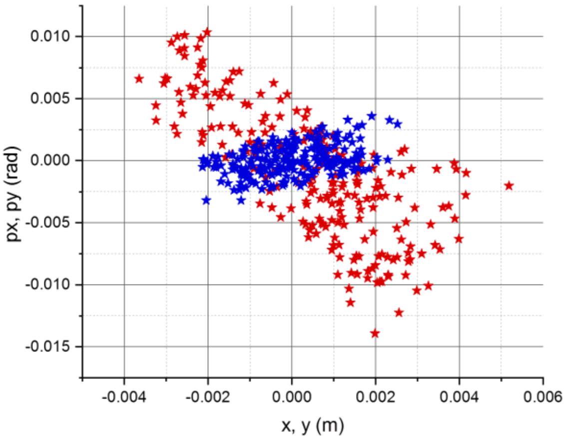

Fig. 17. The beam at the injection channel outlet in radial (red stars) and vertical (blue) planes

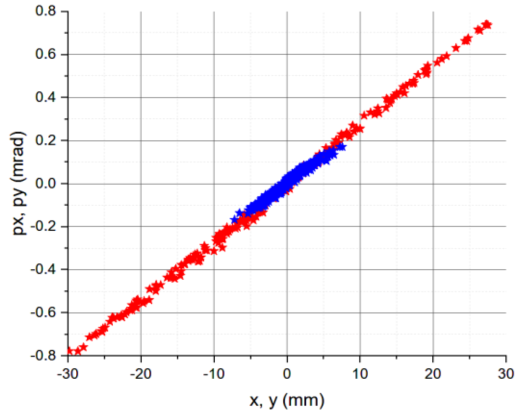

Fig. 18. Beam after the first passage through the of accelerating structures

Thus, the results of modeling the positron beam dynamics show that approximately 1.5% of the described phase volume reaches an energy of 356 MeV.

At an average current of 100 μA and energy of 29 MeV, 2.9 kW of power will be discharged in the converter.

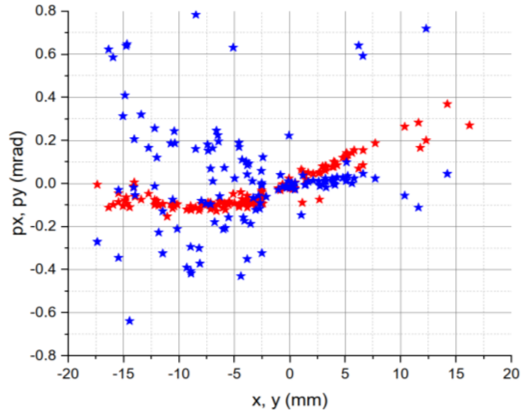

Fig. 19. The beam after the second passage of the accelerating structures (E_{pos} = 356 MeV) in the radial (red stars) and vertical (blue) planes

100 μA corresponds to approximately $6 \cdot 10^{14}$ electrons per second. The conversion factor of electrons into positrons is close to 0.01, so the converter under consideration will generate approximately $6 \cdot 10^{12}$ positrons, of which $9 \cdot 10^{8}$ we will be able to reach the energy of 356 MeV.

The phase portraits of Fig. 18 clearly show the nonlinear effects in the beam dynamics caused by large deviations of the coordinates from the equilibrium ones.

Fig. 20 shows the scheme of positron output on the channels with energy of 181 and 356 MeV.

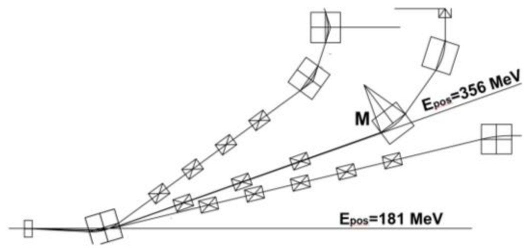

Fig. 20. Positron channel geometry

To bring positrons with an energy of 181 MeV and lower to the experimental setup, a direct channel can be used to transport the electron beam to the neutron source [17].

A positron beam with an energy of 356 MeV hits the beginning of the first arch of the second recirculator ring. The trajectory of the positron beam at the entrance to the magnet M will deviate from the center by 12 mm, which will allow the positrons to be delivered to the experimental setup without building a special channel.

1.3. POSITRON SOURCE FOR SOLID STATE PHYSICS

Paper [14] discusses in detail the methods of using positrons to study the structure of a solid. For these studies, radioactive isotopes are used as positron sources, positrons generated in materials by the interaction of gamma quanta with energies from 1.02 to 15 MeV. A number of techniques require pulsed positron sources with a pulse duration of several picoseconds, which can be provided by accelerators based on the latest technologies [13, 14, 21, 22].

To produce positrons for these purposes, the previously discussed converter can be used on the recirculator [17], which will be installed on one of the channels after the 29 MeV injector (see Fig. 14).

A more detailed spectrum of positrons after the converter in the range below 1 MeV is shown in Fig. 21.

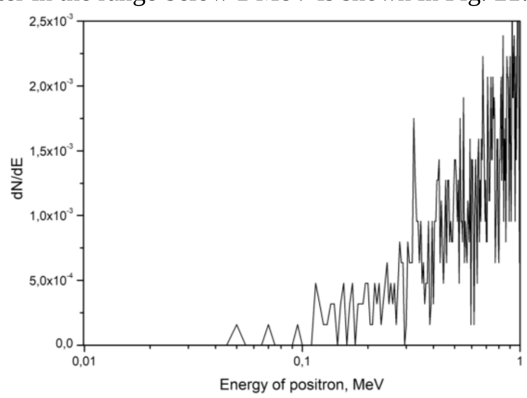

Fig, 21. Positron spectrum

The positron spectrum can be modified both by accelerator technologies [15] and by braking methods [14].

In addition to the use of positrons after the converter, positrons for annihilation in solids can be created by braking gamma quanta that arise when electrons with energy up to 15 MeV interact with massive samples [14].

Modern techniques using positrons produced at superconducting electron accelerators are well described in [13, 14, 16, 21, 22].

CONCLUSIONS

The recycler, the design of which is being developed at KIPT, can create positron beams that make it possible to conduct relevant research in nuclear and solid-state physics.

REFERENCES

1. А.К. Вальтер, И.А. Гришаев, В.В. Еременко и др. Линейный ускоритель электронов на энергию 2 ГэВ // *Труды Международной конференции по ускорителям.* М.: «Атомиздат», 1964, 420 с.

2. V.L. Morokhovskij, G.D. Kovalenko, I.A. Grishaev et al. Channeling of the 1 GeV positrons // *Pis'ma v ZhETF (JETP Letters)*. 1972, v. 16, N 3, p.162-164 (in Russian).

3. D.S. Gemmell. Channeling and related effects in the motion of charged particles through crystals // *Rev. Mod. Phys.* 1973, v. 46, N 1, p. 129-227.

4. A.I. Akhiezer, V.F. Boldyshev, N.F. Shulga. Fast electrons bremsstrahlung on crystal atoms row // *DAN SSSR (Proceedings of the USSR Academy of Sciences)*. 1976, v. 226, N 2, p. 295-297 (in Russian).

5. A.I. Akhiezer, N.F. Shulga. *High-Energy Electrodynamics in Matter*. Gordon and Breach Publishers, 1996, 388 p.

6. N.F. Shul'ga, V.I. Truten', S.P. Fomin. Orientation effects in interaction between high energy particles and chains of atoms in crystal // *ZhETF*. 1984, v. 87, p. 250-256 (in Russian).

7. A.I. Akhiezer, V.I. Truten', N.F. Shul'ga. Stability of motion of high energy particles in crystals and random string approximation // *NIM.* 1992, v. B67, p. 207.

8. G.L. Bochek, V.I. Kulibaba, N.I. Maslov, et al. 1.2 GeV electron radiation spectra in thick tungsten single crystals and total radiation losses in tungsten, germanium and silicon single crystals // *Nucl. Instr. and Meth. in Phys. Res.* 1998, v. B 145, p. 146-149.

9. Г.Л. Бочек, В.И. Витько, Г.Д. Коваленко, Б.И. Шраменко. *Экспериментальные исследования электромагнитных процессов в монокристаллах*. Харьков: ННЦ ХФТИ, 1998, 112 с.

10. M.F. Shul'ga, G.D. Kovalenko, V.B. Ganenko, L.G. Levchuk, S.H. Karpus, I.L. Semisalov. Concept of the state targeted NSC KIPT program of experimental base development for basic and applied research in nuclear and high-energy physics and physics of radiation interaction with matter // *Problems of Atomic Science and Technology. Series "Nuclear Physics Investigations".* 2022, N 3(139), p. 3-6;
https://doi.org/10.46813/2022-139-003

11. F. Tuomisto, I. Makkonen. Defect identification in semiconductors with positron annihilation: experiment and theory // *Reviews of Modern Physics*. 2013, v. 85, p. 583.

12. J. Čížek. Characterization of lattice defects in metallic materials by positron annihilation spectroscopy // *A review. Journal of Materials Science and Technology.* 2018, v. 34, p. 577-98.

13. Positron Annihilation Spectroscopy at the HZDR; https://www.hzdr.de/db/CMS?pNid=363

14. F.A. Selim. Positron annihilation spectroscopy of defects in nuclear and irradiated materials – a review // *Materials Characterization*. April 2021, v. 174, p. 110952;
https://doi.org/10.1016/j.matchar.2021.110952

15. S. Perezhogin, E. Bulyak, V. Mitrochenko, V. Kushnir L, Selivanov'1. Source of positrons on the base of linac LUE-40 KIPT // *PAST*. 2020, N 3(127), p. 7-10.

16. Andreas Wagner et al. *Positron-Annihilation Lifetime Spectroscopy at a Superconducting Electron Accelerator.* SLOPOS 14 Workshop, Matsue, Japan 22-27.5.2016.

17. M.F. Shulga, G.D. Kovalenko, I.S. Guk, P.I. Gladkikh, D.Yu. Shakhov. Optimization of the focusing lattice of the magneto-optical structure of the multifunctional accelerator complex NSC KIPT // *Problems of Atomic Science and Technology*. 2024, N 3(151), p.84-87;
https://doi.org/10.46813/2024-151-050I

18. Chaikovska et al. Positron sources: from conventional to advanced accelerator concepts-based colliders // *Journal of Instrumentation*. 2022, May 2022, v. 17, JINST 17 P05015;
https://doi.org/10.1088/1748-0221/17/05/P05015;

19. J. Teichert et al. Successful user operation of a superconducting radio-frequency photoelectron gun with Mg cathodes // *Phys. Rev. Accel. Beams.* 2021, v. 24, p. 033401.

20. Particle and Heavy Ion Transport code System (PHITS), Ver. 3.20, User's Manual.

21. A. Wagner, M. Butterling, M.O. Liedke, K. Potzger, R. Krause-Rehberg. Positron annihilation lifetime and Doppler broadening spectroscopy at the ELBE facility // *AIP Conference Proceedings*. 2018;1970:040003; DOI:10.1063/1.5040215

22. Andreas Wagner, Positron-Annihilation Lifetime Spectroscopy at a Superconducting Electron Accelerator // *J. Phys.: Conf. Ser.* 2017, v. 791, p. 012004; doi:10.1088/1742-6596/791/1/012004

Article received 25.09.2024

ДЖЕРЕЛА ПОЗИТРОНІВ БАГАТОФУНКЦІОНАЛЬНОГО ПРИСКОРЮВАЛЬНОГО КОМПЛЕКСУ ННЦ ХФТІ

П.І. Гладких, І.С. Гук, Г.Д. Коваленко, О.О. Пархоменко, С.І. Прохорець, Є.В. Рудичев

Розглянуто можливість одержання пучків позитронів на рецеркуляторі електронів, концептуальний проєкт якого розробляється в ННЦ ХФТІ. Проведено оцінки потока позитронів після танталового конвертора. Розрахована ефективність процеса інжекції і прискорення позитронів до енергії 181 і 356 МеВ для експериментів з фізики високих енергій. Розглянуто характеристики пучка для використання у структурних дослідженнях з фізики твердого тіла.